Published for SISSA by Springer

Received: *September 8, 2015*
Revised: *November 5, 2015*
Accepted: *November 16, 2015*
Published: *December 10, 2015*

$N_f = 1$ QCD in external magnetic fields: staggered fermions

Paolo Cea[a,b] **and Leonardo Cosmai**[a]

[a] *INFN, Sezione di Bari,*
Via Amendola 173, I-70126 Bari, Italy
[b] *Dipartimento di Fisica dell'Università di Bari,*
Via Amendola 173, I-70126 Bari, Italy

E-mail: paolo.cea@ba.infn.it, leonardo.cosmai@ba.infn.it

Abstract: We investigate $N_f = 1$ QCD in external magnetic fields on the lattice. The background field is introduced by means of the so-called Schrödinger functional. We adopt standard staggered fermions with constant bare mass $am = 0.025$ and magnetic fields with constant magnetic flux up to $a^2eH \simeq 2.3562$. We find that the the deconfinement and chiral symmetry restoration temperatures do not depend on the strength of the applied magnetic field. Our method allow us to easily study the effects of the external magnetic fields on the QCD thermodynamics. We determine the influences of applied magnetic fields to the free energy, pressure, and equation of state of strongly interacting matter.

Keywords: Nonperturbative Effects, Lattice Quantum Field Theory

ArXiv ePrint: 1509.01982

doi:10.1007/JHEP12(2015)058

JHEP12(2015)058

Contents

JHEP12(2015)058

1 Introduction

Strong interactions are described by quantum chromodynamics (QCD), a local relativistic non-abelian quantum field theory which is not amenable to perturbation theory in the low-energy, large-distance regimes. However, many fundamental questions are linked to the large scale behavior of QCD. In particular, non-perturbative approaches to QCD can be used to account for the different phases of hadronic matter under extreme conditions.

Recently, the study of the effects of strong magnetic fields on the QCD phase diagram has become a topic of increasing interest (for a recent review, see refs. [1, 2]). In the non-perturbative regimes this problem can be efficiently approached by lattice QCD simulations with dynamical quarks.

The study of lattice gauge theories with external background fields has been pioneered in refs. [3, 4] for the U(1) Higgs model in an external electromagnetic field. In the continuum a background field can be introduced by writing:

$$A_\mu(x) \to A_\mu(x) + A^{\rm ext}_\mu(x)\,. \tag{1.1}$$

In the lattice approach one deals with link variables $U_\mu(x)$. Accordingly, on the lattice eq. (1.1) becomes:

$$U_\mu(x) \to U_\mu(x)\, U^{\rm ext}_\mu(x)\,, \tag{1.2}$$

where $U^{\rm ext}_\mu(x)$ is the lattice version of the background field $A^{\rm ext}_\mu(x)$. As a consequence the lattice action gets modified as:

$$S[U] \to S[U] + \delta\, S[U, U^{\rm ext}]\,, \tag{1.3}$$

where $\delta S[U, U^{\rm ext}]$ takes into account the influence of the external field. An alternative method, which is equivalent in the continuum limit, is based on the observation that an external background field can be introduced via an external current [5, 6]:

$$J_\mu^{\rm ext} = \partial_\nu F_{\nu\mu}^{\rm ext}, \tag{1.4}$$

so that the action gets modified as:

$$S \to S + S_B\,, \tag{1.5}$$

where:

$$S_B = \int dx\, J_\mu^{\rm ext}(x)\, A_\mu(x) = -\frac{1}{2}\int dx\, F_{\nu\mu}^{\rm ext}(x)\, F_{\nu\mu}(x)\,. \tag{1.6}$$

The main disadvantage of these approaches resides on the lack of gauge invariance for non-abelian gauge theories. The issue of gauge invariance, however, does not pose if one is interested in QCD in external magnetic fields. In fact, let us consider the lattice partition function of QCD with f flavors of dynamical staggered quarks:

$$Z = \int \mathcal{D}U\, e^{-S_G} \prod_f [\det M(U)]^{\frac{1}{4}}, \tag{1.7}$$

where S_G is the gauge field action and M is the fermion matrix for a staggered quark with bare mass am_f:

$$\begin{aligned} M_{n,m}(U) &= \sum_{\nu=1}^{4} \frac{\eta_\nu(n)}{2}\left\{U_\nu(n)\delta_{m,n+\hat{\nu}} - U_\nu^\dagger(m)\delta_{m,n-\hat{\nu}}\right\} + am_f\,\delta_{m,n}\,, \\ \eta_\nu(n) &= (-1)^{n_1+\ldots+n_{\nu-1}}\,. \end{aligned} \tag{1.8}$$

Since magnetic fields couple only to quarks, external magnetic fields can be introduced in the lattice action by replacing in the fermion mass matrix eq. (1.8) the gauge field links according to eq. (1.2), where the $U_\mu^{\rm ext}(x)$'s are U(1) elements corresponding to the external magnetic fields with continuum gauge potential $A_\mu^{\rm ext}(x)$. For instance, if we consider constant magnetic fields directed along the x_3 direction, then the continuum gauge potential in the Landau gauge reads:

$$A_k^{\rm ext}(\vec{x}) = \delta_{k,2}\, x_1 H\,. \tag{1.9}$$

Therefore, we may write:

$$U_1^{\rm ext}(\vec{x}) = U_3^{\rm ext}(\vec{x}) = U_4^{\rm ext}(\vec{x}) = 1\,, \qquad U_2^{\rm ext}(\vec{x}) = \cos(q_f e H x_1) + i\sin(q_f e H x_1)\,, \tag{1.10}$$

where e is the (positive) elementary charge and q_f is the quark charge ($q_u = 2/3$, $q_d = -1/3$). Since the lattices have the topology of a torus, the magnetic field turns out to be quantized [4]:

$$a^2 q_f\, eH = \frac{2\pi}{L_s^2}\, n_{\rm ext}\,, \quad n_{\rm ext} \text{ integer} \tag{1.11}$$

where L_s is the lattice spatial size. Indeed, in the recent literature this approach has been adopted in extensive numerical simulations of QCD in external magnetic fields [7–23].

JHEP12(2015)058

An alterative approach to put background fields on the lattice has been proposed since long time [24]. Indeed, that proposal allows to overcome the problem of gauge invariance by implementing background fields on the lattice by means of the manifestly gauge-invariant lattice Schrödinger functional. In this paper we present an exploratory study of lattice QCD immersed in a uniform external magnetic field. The background field is introduced by using the Schrödinger functional. Moreover, for simplicity, we restrict ourself to one flavor of staggered dynamical quark.

The plan of the paper is as follows. In section 2, for completeness, we briefly discuss our method to introduce background fields on the lattice. In section 3 we present the results of our numerical simulations for several local observables. We also address the problem of the possible dependence of the pseudoritical couplings on the magnetic field strengths. Section 4 is devoted to the discussion of the effects of magnetic fields on QCD thermodynamics. Finally, our conclusions are relegated in section 5.

2 Magnetic fields within the Schrödinger functional

For reader's convenience, let us briefly review background fields in lattice gauge theories within the Schrödinger functional. Firstly, we illustrate the method in pure gauge theories. In ref. [24], to overcome the gauge invariance problem in presence of background fields, it was proposed that background fields on the lattice could be implemented by means of the gauge invariant lattice Schrödinger functional:

$$\mathcal{Z}[U_k^{\rm ext}] = \int \mathcal{D}U\, e^{-S_G}, \tag{2.1}$$

where the functional integration is extended over links on a lattice with the hypertorus geometry and satisfying the constraints ($x_t \equiv x_4$ is the temporal coordinate)

$$U_k(x)|_{x_t=0} = U_k^{\rm ext}(\vec{x})\,, \quad (k=1,2,3)\,. \tag{2.2}$$

One also imposes that links at the spatial boundaries are fixed according to eq. (2.2). In fact, in the continuum this last condition amounts to the requirement that fluctuations over the background field vanish at infinity. This approach has been applied for both abelian and non-abelian gauge theories with different background fields [25–34].

The effects of dynamical fermions can be accounted for quite easily. Indeed, when including dynamical fermions, the lattice Schrödinger functional in presence of a static external background gauge field becomes:

$$\begin{aligned}\mathcal{Z}[U_k^{\rm ext}] &= \int_{U_k(L_t,\vec{x})=U_k(0,\vec{x})=U_k^{\rm ext}(\vec{x})} \mathcal{D}U\, \mathcal{D}\psi\, \mathcal{D}\bar{\psi} e^{-(S_G+S_F)} \\ &= \int_{U_k(L_t,\vec{x})=U_k(0,\vec{x})=U_k^{\rm ext}(\vec{x})} \mathcal{D}U e^{-S_G}\, \det M\,,\end{aligned} \tag{2.3}$$

where S_F is the fermion action and M indicates the generic fermion matrix. Notice that the fermion fields are not constrained and the integration constraint is only relative to the gauge fields. This leads to the appearance of the gauge invariant fermion determinant after

JHEP12(2015)058

integration on the fermion fields. As usual we impose on fermion fields periodic boundary conditions in the spatial directions and anti-periodic boundary conditions in the temporal direction. In fact, eq. (2.3) has been employed to study the dynamics of QCD with two degenerate staggered quarks [35, 36], as well as the quantum Hall effect in graphene [37].

In the case of QCD in constant magnetic fields the constraints in the lattice Schrödinger functional need to be slightly modified to take into account that the magnetic field is coupled only to quarks. To this end, we impose that during the upgrade of the gauge links $U_k^{\rm ext}(\vec{x}) = \mathbb{I}$, while for the upgrade of the fermion fields $U_k^{\rm ext}(\vec{x}) = \mathbb{I} \times e^{i\theta_k^{\rm ext}(\vec{x})}$ where:

$$\theta_k^{\rm ext}(\vec{x}) = \delta_{k,2}\, q_f\, eH\, x_1\,. \tag{2.4}$$

Since our Schrödinger functional $\mathcal{Z}[U_k^{\rm ext}]$ is defined on a lattice with periodic boundary conditions, usually we impose that:

$$\theta_2(x_1, x_2, x_3, x_4) = \theta_2(x_1 + L_s, x_2, x_3, x_4)\,. \tag{2.5}$$

As a consequence the magnetic field H turns out to be quantized:

$$a^2 q_f\, eH = \frac{2\pi}{L_s}\, n_{\rm ext} \tag{2.6}$$

with $n_{\rm ext}$ integer. However, it should be kept in mind that we are dealing with a periodic lattice with fixed boundary conditions, so that is is not strictly necessary to impose the quantization eq. (2.6) and the "integer" $n_{\rm ext}$ can be an arbitrary real number.

3 Numerical results

We perform simulations of lattice QCD with one-flavor of rooted staggered quark. Our numerical results were obtained by choosing as gauge action the Wilson action:

$$S_G = \beta\, S_W \equiv \beta \sum_{x,\mu>\nu} \left(1 - \frac{1}{3}\,{\rm Re}[{\rm Tr}\, U_{\mu\nu}(x)]\right) \tag{3.1}$$

where $U_{\mu\nu}(x)$ are the plaquettes in the (μ,ν)-plane and $\beta = \frac{6}{g^2}$. Therefore we are led to consider the following lattice Schrödinger functional:

$$\mathcal{Z}[U_k^{\rm ext}] = \int_{U_k(L_t,\vec{x})=U_k(0,\vec{x})=U_k^{\rm ext}(\vec{x})} \mathcal{D}U\, e^{-\beta S_W}\, [\det M(U)]^{\frac{1}{4}}\,, \tag{3.2}$$

where the staggered fermion matrix is given by eq. (1.8). To perform the functional integration over the SU(3) links we have made use of the publicly available MILC code [38] which has been suitably modified by us in order to introduce the boundary constraints eq. (2.2). All simulations make use of the rational hybrid Monte Carlo (RHMC) algorithm. The functional integration is performed over the lattice links, but the links at the spatial boundaries are fixed according to eq. (2.2). Accordingly, the links which are frozen are not evolved during the molecular dynamics trajectory and the corresponding conjugate momenta are set to zero. The length of each RHMC trajectory has been set to 1.0 in molecular dynamics time units. For each value of the gauge coupling β and the magnetic field

JHEP12(2015)058

eH we collected 4000–5000 trajectories, and about 10000 trajectories around the critical coupling. To allow thermalization we typically discarded 1000 trajectories. The statistical errors were estimated by means of boostrap combined with binning.

In the present exploratory study we consider lattices of size $L_s = 24$ and $L_t = 4$ and fixed bare fermion mass $m_0 \equiv am = 0.025$. At fixed L_t the temperature of the gauge system $T = \frac{1}{aL_t}$ is changed by varying the coupling constant β.

Since the smallest quark electric charge is $|q| = 1/3$, from eq. (2.6) we get:

$$a^2\, eH = \frac{6\pi}{L_s}\, n_{\rm ext} \tag{3.3}$$

Different strengths of the external magnetic field are labelled by the parameter $n_{\rm ext}$ according to eq. (3.3). We performed simulations for $n_{\rm ext} = 0, 1, 3$, corresponding to field strength $a^2eH = 0, 0.7854, 2.3562$ in lattice units, and assumed $q_f = \frac{2}{3}$ (up quark). Note that, the case of down quark $q_f = -\frac{1}{3}$ can be recovered with $n_{\rm ext} = -\frac{1}{2}$ ($a^2eH = -0.3927$). In fact, to check the dependence of the free energy on the magnetic field we have also performed numerical simulations for $n_{\rm ext} = -\frac{1}{2}$.

For the sake of completeness let us discuss, briefly, how the background magnetic field influences the dynamics of the gauge system. We said that to update the gauge system we used the rational hybrid Monte Carlo algorithm. As it is well known (see for instance ref. [39]), to simulate the fermion determinant one introduces color-triplet scalar pseudofermion fields. The pseudofermion action depends on the inverse of the staggered fermion matrix eq. (1.8). In the molecular dynamics one solves the equations of motion of the momenta conjugated to the gauge links. The derivative of the gauge momentum is called the force term, which is the formal derivative of the effective action with respect to the gauge potential. Thus, the force term consists of two contributions, namely the gauge force term and the fermion force term. Our boundary conditions correspond to set $U_k^{\rm ext} = \mathbb{I}$ on the $x_t = 0$ hypersurface and at the spatial boundaries of the lattice in the gauge force term, while $U_k^{\rm ext}(\vec{x}) = \mathbb{I} \times e^{i\theta_k^{\rm ext}(\vec{x})}$ in the fermion force term. To maintain the above constraints during the molecular dynamics, the momenta conjugated to the frozen gauge links are set to zero.

3.1 Local observables

In this section we are interested in the effects of the external magnetic field on several local observables. First, we consider the gauge action which, following the MILC convention, we define as:

$$G_{\rm action} = \frac{1}{L_s^3\, L_t} \left\langle \sum_{x,\mu>\nu} \left[3 - {\rm Re\,Tr}\, U_{\mu\nu}(x)\right] \right\rangle . \tag{3.4}$$

In figure 1 we display the gauge action as a function on the gauge coupling β for three different values of the magnetic field. Since $G_{\rm action}$ is a pure gauge quantity, it couples to the magnetic field only through quark loops. Therefore we expect that this quantity should manifest a very weak dependence on the magnetic field. Indeed, figure 1 shows that the effects of the magnetic field on the gauge action are at most of order 10^{-2} (see figure 5). Interestingly enough, we see that the gauge action increases as a function of eH in the

JHEP12(2015)058

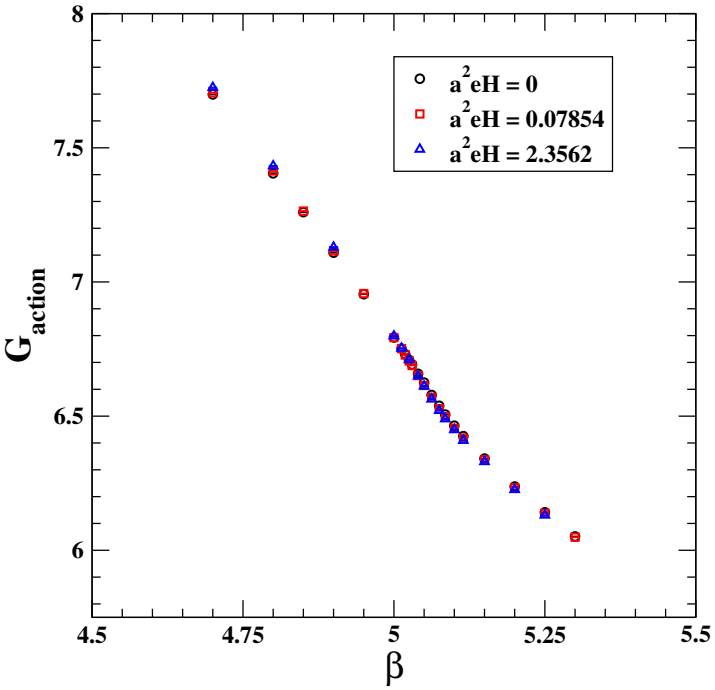

Figure 1. The gauge action eq. (3.4) versus β for $q_f = \frac{2}{3}$ and $n_{\rm ext} = 0, 1, 3$.

strong coupling region whereas it decreases in the weak coupling region. In fact the three different curves displayed in figure 1 cross near the critical coupling $\beta_c \simeq 5.0$.

A more interesting quantity is the quark chiral condensate:

$$\langle \overline{\psi}\,\psi \rangle = \frac{1}{L_s^3\, L_t}\, \frac{1}{4}\, \langle \mathrm{Tr}\, M^{-1} \rangle\,, \tag{3.5}$$

which should display a pronunciate dependence on the magnetic field. In figure 2 we display $\langle \overline{\psi}\,\psi \rangle$ versus the gauge coupling β for three different values of the magnetic field eH. The chiral condensate was computed by noise estimators with 4 random vectors. It is evident that the chiral condensate increases as a function of eH for all temperatures. For comparison, in figure 2 we also display the real part of the Polyakov loop expectation value:

$$\langle L \rangle = \frac{1}{3\, L_s^3} \Big\langle \sum_{\vec{x}} \prod_{x_t=0}^{L_t} \mathrm{Tr}\, U_4(\vec{x}, x_t) \Big\rangle\,. \tag{3.6}$$

The Polyakov loop L, likewise the gauge action, is a pure gauge observable. Nevertheless, figure 2 shows that the Polyakov loop displays a sizable dependence on the magnetic field. In particular, we see that L increases with eH for all temperatures as for the chiral condensate. This behavior can be qualitatively understood if the quark free energy decreases with the applied magnetic field. In fact, later on we will show that the strongly interacting system behaves like a paramagnetic medium, i.e. positive magnetic susceptibility.

Another interesting feature of figure 2 is the crossing of the chiral condensate and the Polyakov loop near the critical temperature. In fact, figure 2 seems to suggest that the

JHEP12(2015)058

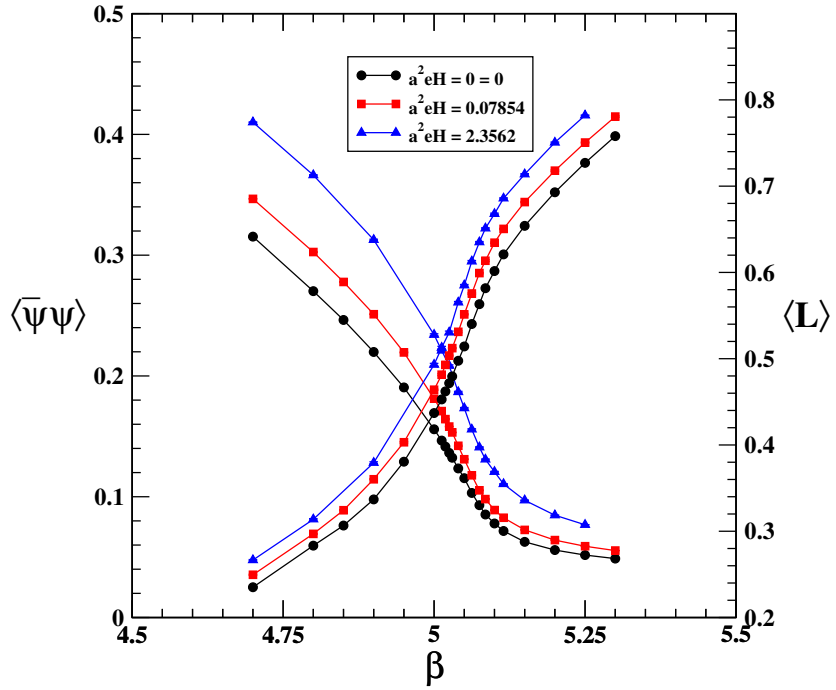

Figure 2. The chiral condensate eq. (3.5) (left) and the real value of the Polyakov loop eq. (3.6) (right) versus β for $q_f = \frac{2}{3}$ and $n_{\rm ext} = 0, 1, 3$.

pseudocritical gauge coupling β_c does not manifest a strong dependence on the magnetic field eH.

3.2 Pseudocritical couplings

In this section we address the problem of the possible dependence of the pseudocritical coupling on the magnetic field. In general, the (pseudo)critical coupling is determined as the value for which some relevant susceptibilities exhibit a peak. In the present paper, to precisely localize the peak in the relevant susceptivity we parametrize the peak region with a Lorentzian function:

$$F(\beta) = \frac{a_1}{a_2\,(\beta - \beta_c)^2 + 1}\,. \tag{3.7}$$

Our estimate of the critical coupling β_c is obtained by fitting the susceptivity to eq. (3.7) in the peak region. We use the Polyakov loop susceptibility as well as the disconnected part of the chiral susceptibility to locate the transition temperature to the high temperature phase of QCD.

First, we consider the disconnected chiral susceptibility:

$$\chi^{\rm disc}_{\bar\psi\psi} = \frac{1}{L_s^3\,L_t}\,\frac{1}{16}\left(\langle[{\rm Tr}\,M^{-1}]^2\rangle - [\langle{\rm Tr}\,M^{-1}\rangle]^2\right). \tag{3.8}$$

In figure 3 we show the disconnected chiral susceptibility as a function of the gauge coupling for three different values of eH. As usual the disconnected chiral susceptibility displays a sharp peak near the chiral critical coupling. Interestingly enough, the dependence of the

JHEP12(2015)058

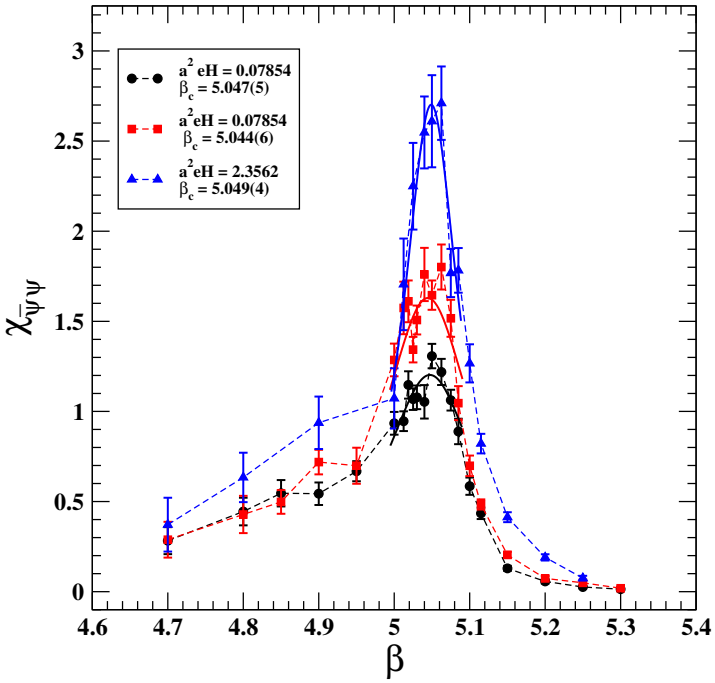

Figure 3. The disconnected chiral susceptibility eq. (3.8) versus β for $q_f = \frac{2}{3}$ and $n_{\rm ext} = 0, 1, 3$. The continuous lines are the results of the fits of the chiral susceptibilities to eq. (3.7). The estimate critical couplings are reported in the legend.

chiral susceptibility on the magnetic field is almost relegated to the peak region. Moreover, the peak values increase with eH signaling that the chiral transition sharpens in presence of a non-zero magnetic field. Notwithstanding, we find that, within our statistical uncertainties, the chiral critical coupling does not depend on the magnetic field.

We have also considered the Polyakov loop susceptibility:

$$\chi_L = L_s^3 \left(\langle L^2 \rangle - \langle L \rangle^2 \right) . \tag{3.9}$$

Results for the Polyakov loop susceptibility are shown in figure 4. In this case we see that the dependence of the Polyakov loop susceptibility on the magnetic field is less pronounced with respect to the disconnected chiral susceptibility. Moreover, figure 4 shows that the peak of χ_L decreases with increasing eH. This means that the applied magnetic field tends to smooth out the deconfinement transition. However, even in this case the deconfinement critical couplings does not display any appreciable dependence on eH. Moreover, we find that the chiral and deconfinemnet critical couplings agree for any values of the magnetic field strengths considered in this work. Finally, as further check, we have considered the variation of the gauge action:

$$\Delta G_{\rm action} \equiv G_{\rm action}(eH \neq 0) - G_{\rm action}(eH = 0) , \tag{3.10}$$

which is known to display a peak in the critical region. Of course, by using $\Delta G_{\rm action}$ we may estimate the pseudocritical couplings only for non-zero magnetic field strengths.

JHEP12(2015)058

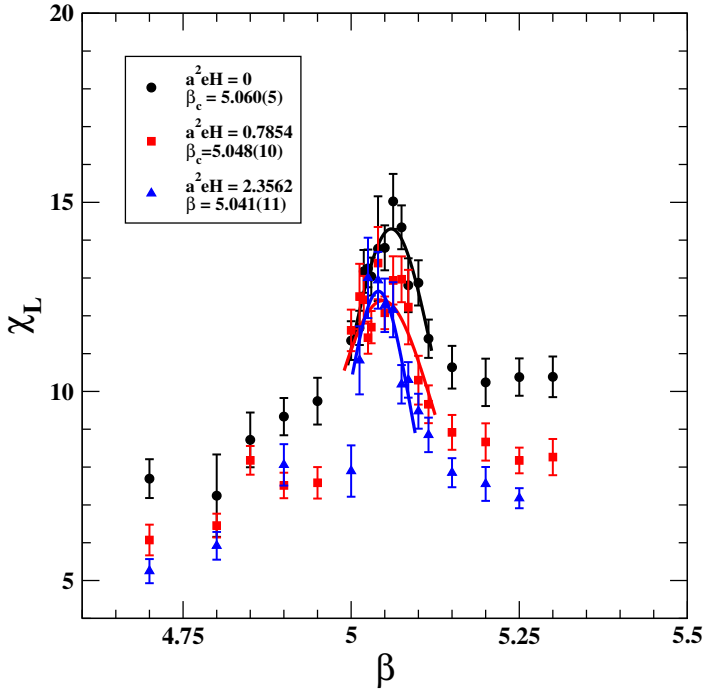

Figure 4. The Polyakov loop susceptibility eq. (3.9) versus β for $q_f = \frac{2}{3}$ and $n_{\rm ext} = 0, 1, 3$. The continuous lines are the results of the fits of the Polyakov loop susceptibilities to eq. (3.7). The estimate critical couplings are reported in the legend.

In figure 5 we show $\Delta G_{\rm action}$ versus β for the three different values of the magnetic field employed in the present work. As discussed in section 3.1 the effects of the magnetic field on the gauge action are tiny. Moreover, the non monotonic dependence of the gauge action on eH is clearly displayed in figure 5. In any case, we see that $\Delta G_{\rm action}$ does display a well developed peak in the critical region. We find that the peaks in $\Delta G_{\rm action}$ are located at a systematically slightly larger values of the gauge coupling with respect to the chiral and Polyakov loop susceptibilities. In a finite volume this is, of course, not unexpected. Indeed, we recall that we are using lattices with fixed boundary conditions and, as previous studies showed, the gauge action turns out to be more susceptible to finite volume effects. Nonetheless, what it is relevant is that the pseudocritical couplings do not depend on the magnetic field eH.

For reader convenience, in table 1 we summarize our estimates of the critical couplings β_c as function of the magnetic field eH. From table 1 we may safely conclude that the critical temperature does not depend on the external magnetic field.

4 Thermodynamics in external magnetic fields

The partition function $\mathcal{Z}[U_k^{\rm ext}]$ allows us to define observables that can be used to establish the equation of state of the theory. Such observables play an important role in describing the thermodynamic properties of the system.

JHEP12(2015)058

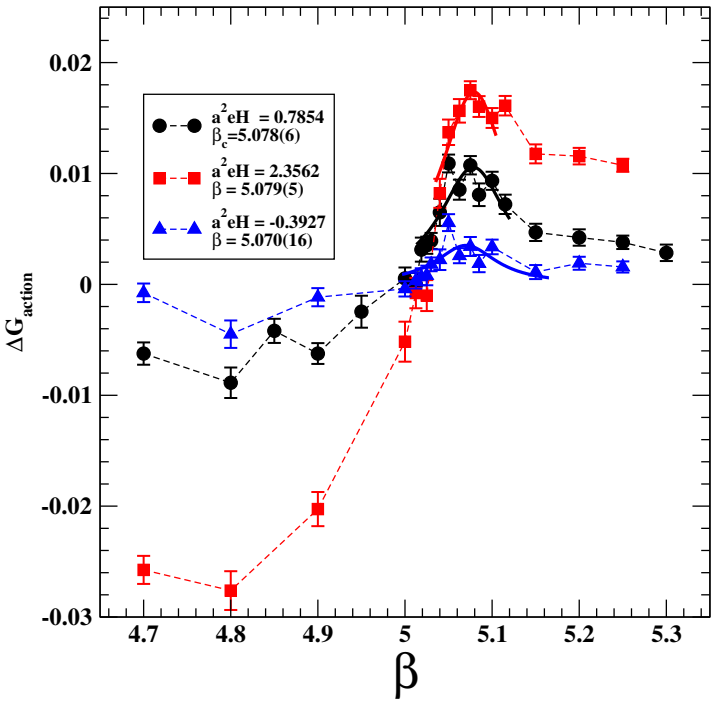

Figure 5. $\Delta G_{\rm action}$ eq. (3.9) versus β for $q_f = \frac{2}{3}$ $n_{\rm ext} = 1, 3$, and $q_f = -\frac{1}{3}$ $n_{\rm ext} = 1$. The continuous lines are the results of the fits of $\Delta G_{\rm action}$ to eq. (3.7). The estimate critical couplings are reported in the legend.

The free energy density is related to the logarithm of the partition function as:

$$f(T,H) = -\frac{T}{V}\,\log \mathcal{Z}[U_k^{\rm ext}] = -\frac{1}{L_s^3\,L_t}\,\log \mathcal{Z}[U_k^{\rm ext}]\,. \tag{4.1}$$

The pressure is given by the derivative of $T \log \mathcal{Z}[U_k^{\rm ext}]$ with respect to the volume. Assuming that we have a large, homogeneous system, differentiation with respect to V is equivalent to dividing by the volume. Therefore in the thermodynamic limit the pressure can be written as minus the free energy density:

$$p(T,H) = -f(T,H)\,. \tag{4.2}$$

Using the well-known relation between the trace anomaly (also called interaction measure) and the derivative of the pressure:

$$I(T,H) = \varepsilon(T,H) - 3\,p(T,H) = T^5\,\frac{\partial}{\partial T}\,\frac{p(T,H)}{T^4}\,, \tag{4.3}$$

one can easily calculate the energy density:

$$\varepsilon(T,H) = I(T,H) + 3\,p(T,H)\,, \tag{4.4}$$

the entropy density:

$$s(T,H) = \frac{\varepsilon(T,H) + p(T,H)}{T}\,, \tag{4.5}$$

JHEP12(2015)058

Operator	a^2eH	β_c
$\chi^{\rm disc}_{\bar\psi\psi}$	0	5.047(5)
	0.7854	5.044(6)
	2.3562	5.049(4)
	−0.3927	5.046(2)
χ_L	0	5.060(5)
	0.7854	5.048(10)
	2.3562	5.041(11)
	−0.3927	5.051(5)
$\Delta G_{\rm action}$	0	–
	0.7854	5.078(6)
	2.3562	5.079(5)
	−0.3927	5.070(16)

Table 1. Summary of the values of the critical couplings β_c estimated with different operators for the magnetic field strenghts considered in this work.

and the speed of sound:

$$c_s^2 = \left.\frac{\partial p}{\partial \varepsilon}\right|_s . \tag{4.6}$$

As usual, we need to renormalize the free energy density by subtracting the divergent zero-point energy. To do this it is enough to subtract the zero temperature contribution. Thus we define:

$$f_r(T,H) = f(T,H) - f(0,H)\,, \qquad p_r(T,H) = -f_r(T,H)\,. \tag{4.7}$$

The zero temperature contributions are conventionally obtained by performing simulations on lattices with $L_t = L_s$. Moreover, since we are interested in the thermal magnetic properties of our system, we will focus on:

$$\Delta f_r(T,H) \equiv f_r(T,H) - f_r(T,H=0)\,, \qquad \Delta p_r(T,H) = -\Delta f_r(T,H)\,. \tag{4.8}$$

In a Monte Carlo simulation, one cannot compute the partition function directly. The most frequently used method in practice is the integral method, in which a derivative of the free energy with respect to some parameter serves as observable, which then gets integrated again to yield the free energy density. Since we are doing simulations at fixed L_t, it is convenient to take derivatives with respect to the bare gauge coupling β. The expectation values of the derivatives with respect to β of our partition function correspond to the average Wilson action. Thus, we have:

$$\frac{1}{T^4}\frac{\partial \Delta p_r(T,H)}{\partial \beta} = -\frac{L_t^3}{L_s^3}\Big\{\big(\langle S_W\rangle_{H,T} - \langle S_W\rangle_{H,0}\big) - \big(\langle S_W\rangle_{H=0,T} - \langle S_W\rangle_{H=0,0}\big)\Big\}\,. \tag{4.9}$$

In figure 6 we report our results for the β-derivative of $\Delta p_r(T,H)$ (normalized to T^4) versus the ratio T/T_c for three different values of the magnetic field. We recall that the temperature corresponding to a given value of the gauge coupling is given by the relation

JHEP12(2015)058

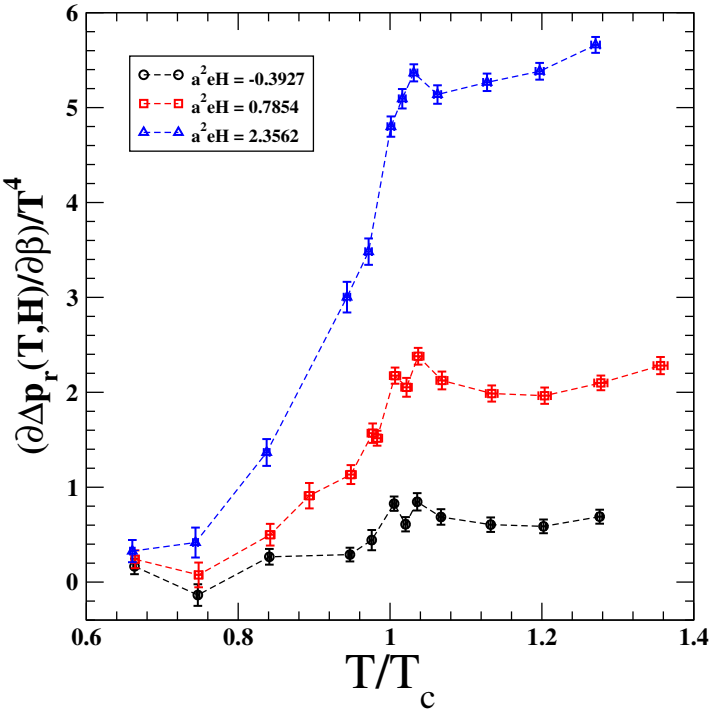

Figure 6. $\frac{1}{T^4}\frac{\partial \Delta p_r(T,H)}{\partial \beta}$, eq. (4.9), versus T/T_c for $q_f = \frac{2}{3}$ $n_{\rm ext} = 1, 3$, and $q_f = -\frac{1}{3}$ $n_{\rm ext} = 1$.

$T = \frac{1}{L_t a(\beta)}$. For the dependence of the lattice spacing on the gauge coupling we used the two-loop β-function. Accordingly, we have:

$$a(\beta)\,\Lambda_{\rm QCD} = f_{\rm QCD}(\beta)\,, \tag{4.10}$$

where $f_{\rm QCD}(\beta)$ is the asymptotic scaling function of QCD with one dynamical fermion $N_f = 1$:

$$f_{\rm QCD}(\beta) = \left(\frac{6b_0}{\beta}\right)^{-b_1/(2b_0^2)} \exp\left(-\frac{\beta}{12b_0}\right), \qquad b_0 = \frac{11 - \frac{2}{3}N_f}{(4\pi)^2}\,, \qquad b_1 = \frac{102 - \frac{38}{3}N_f}{(4\pi)^4}\,. \tag{4.11}$$

For definitiveness, the critical temperatures have been obtained by using the pseudocritical gauge coupling estimated by means of the chiral susceptibilities. Obviously, a direct determination of the physical scale should be preferable. However, it is known that the lattice violations to the asymptotic scaling law eq. (4.10) are within a few percent. So that, the adopted approximation is adequate to the purpose of the present exploratory study.

From the derivative of the pressure, after numerical integration, we may easily obtain $\Delta p_r(T,H) = -\Delta f_r(T,H)$. In figure 7 we display the normalized pressure $\Delta p_r(T,H)$ versus the temperature for three different values of the magnetic field. Figure 7 shows that the magnetic contributions to the renormalized pressure is clearly different from zero even for $T < T_c$, and it seems to vanish rapidly for low temperatures. This behavior can be naturally accounted for within the Hadron Resonance Gas model (see, for instance, ref. [40, 41]). On the other hand, for temperatures above the critical temperature the pressure increases

JHEP12(2015)058

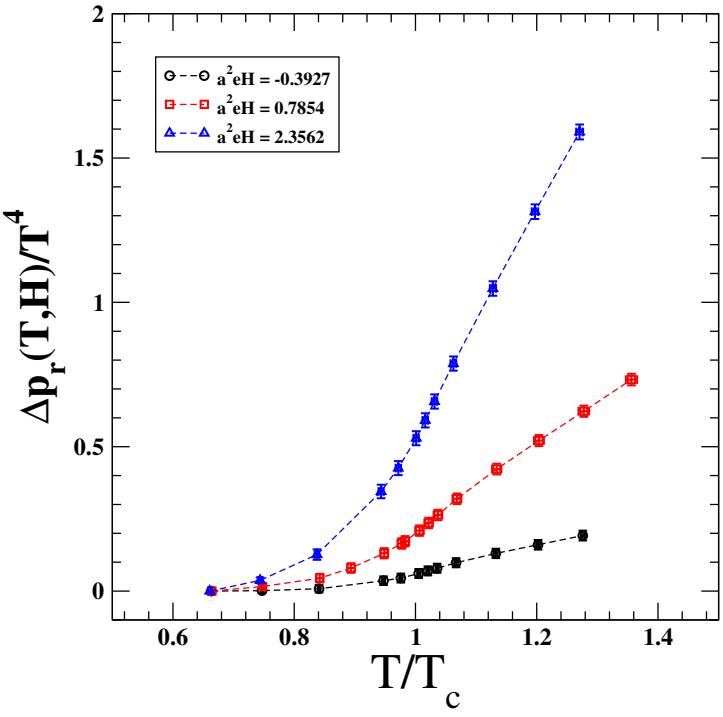

Figure 7. $\frac{\Delta p_r(T,H)}{T^4}$ versus T/T_c for $q_f = \frac{2}{3}$ $n_{\rm ext} = 1, 3$, and $q_f = -\frac{1}{3}$ $n_{\rm ext} = 1$.

rapidly in qualitative agreements with perturbative calculations in the high-temperature regime [42].

As concern the energy density, using eq. (4.3) we may write:

$$\frac{I(T,H)}{T^4} = \frac{\Delta\varepsilon_r(T,H) - 3\,\Delta p_r(T,H)}{T^4} = T\,\frac{d\,\beta}{d\,T}\,\frac{\partial}{\partial\beta}\left[\frac{\Delta p_r(T,H)}{T^4}\right], \tag{4.12}$$

$$T\,\frac{d\,\beta}{d\,T} = -a\,\frac{d\,\beta}{d\,a} \equiv R_\beta(\beta)\,, \tag{4.13}$$

where $R_\beta(\beta)$ is the lattice $\beta_{\rm QCD}$-function. According to our approximation, we have:

$$R_\beta(\beta) = -\frac{f_{\rm QCD}(\beta)}{\frac{d}{d\,\beta} f_{\rm QCD}(\beta)}\,. \tag{4.14}$$

Using eqs. (4.12), (4.13), and (4.14) we determined the so-called interaction measure displayed in figure 8 for three different values of the magnetic field.

After that, the magnetic contributions to the renormalized energy density can be straightforwardly obtained as:

$$\frac{\Delta\varepsilon_r(T,H)}{T^4} = \frac{\Delta I(T,H)}{T^4} + 3\,\frac{\Delta p_r(T,H)}{T^4}\,. \tag{4.15}$$

In figure 9 we show the renormalized energy density. Even for the magnetic contribution to the energy density we find two different regimes for $T < T_c$ (confined phase) and $T > T_c$ (deconfined phase). Having determined the magnetic contribution to the pressure and

JHEP12(2015)058

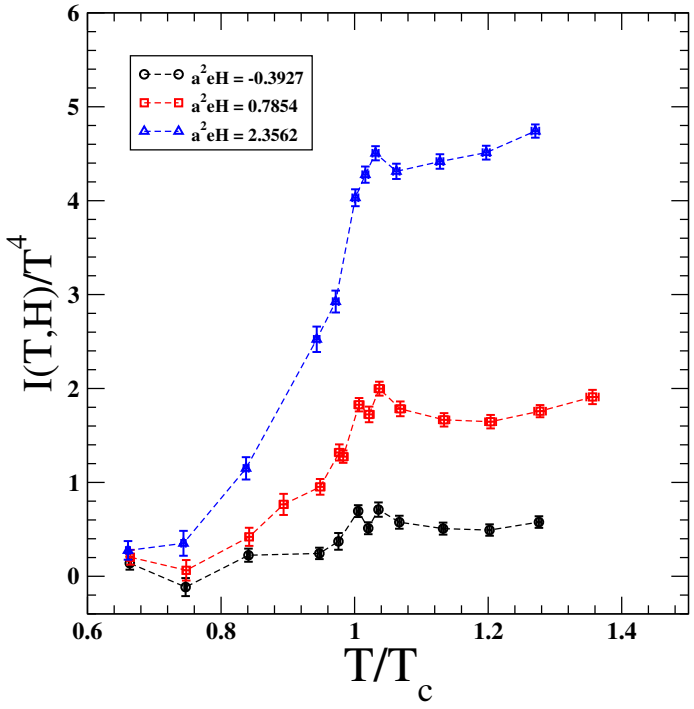

Figure 8. The interaction measure $\frac{I(T,H)}{T^4}$, eq. (4.12), versus T/T_c for $q_f = \frac{2}{3}$ $n_{\rm ext} = 1, 3$, and $q_f = -\frac{1}{3}$ $n_{\rm ext} = 1$.

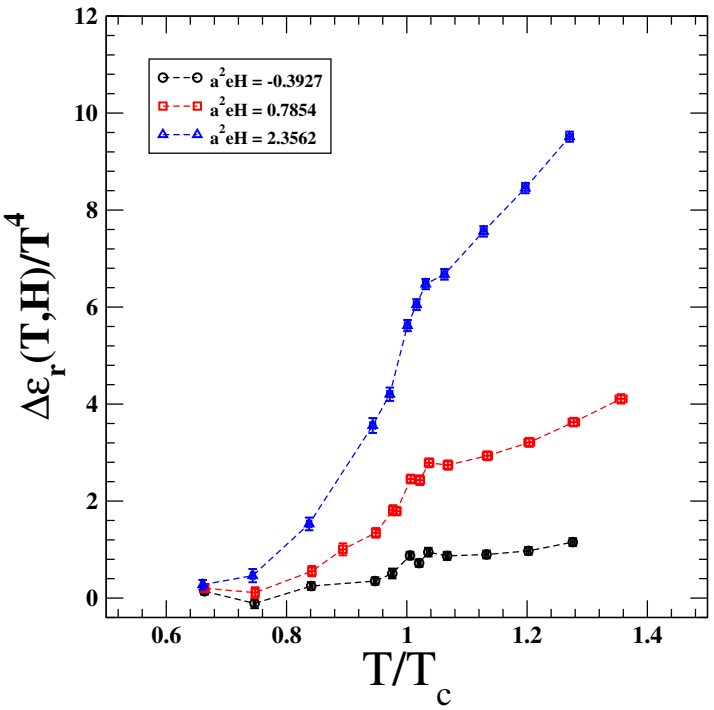

Figure 9. $\frac{\Delta\varepsilon_r(T,H)}{T^4}$, eq. (4.15), versus T/T_c for $q_f = \frac{2}{3}$ $n_{\rm ext} = 1, 3$, and $q_f = -\frac{1}{3}$ $n_{\rm ext} = 1$.

JHEP12(2015)058

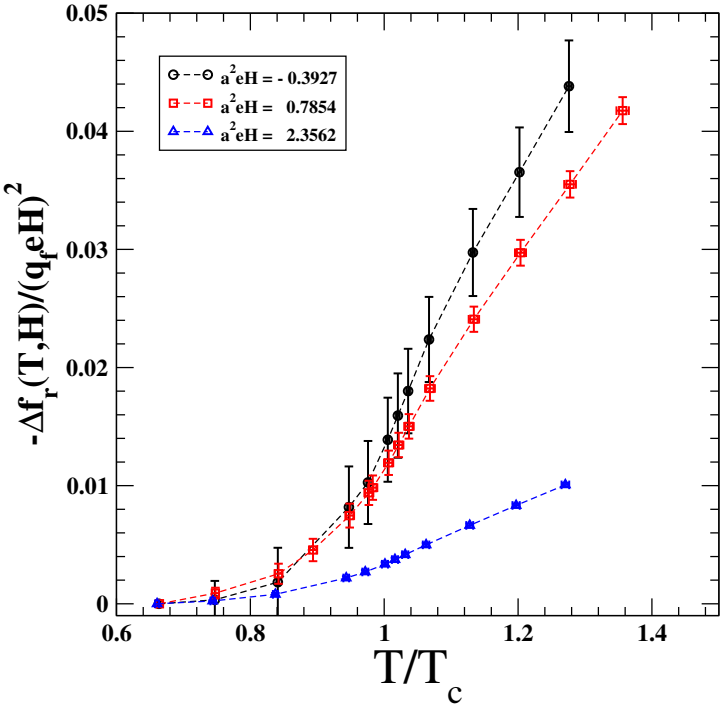

Figure 10. $\frac{\Delta f_r(T,H)}{(q_f eH)^2}$ versus T/T_c for $q_f = -\frac{1}{3}$ $n_{\rm ext} = 1$, and $q_f = \frac{2}{3}$ $n_{\rm ext} = 1, 3$.

energy density, in principle one can construct the equation of state and obtain the entropy density and the speed of sound by means of eqs. (4.5) and (4.6). For the purposes of the present paper we do not discuss any further this matter. We, merely, observe that in the deconfined phase $T > T_c$ the magnetic contribute to the energy density increases slower with respect to the pressure by increasing the temperature. This behavior leads to a stiffening of the equation of state.

Let us, finally, address the problem of the magnetic susceptibility. As is well known, for small magnetic field strengths we may write for the free energy density (see, for instance, ref. [43]):

$$\Delta f_r(T, H) = -\frac{1}{2}\,\chi_{\rm mag}(T)\,H^2, \tag{4.16}$$

where $\chi_{\rm mag}$ is the magnetic susceptibility. Therefore, to determine the magnetic susceptibility we need to check if $\Delta f_r(T, H) = -\Delta p_r(T, H)$ scales with H^2 at least for small enough magnetic field strengths. To this end, in figure 10 we display $\frac{\Delta f_r(T,H)}{(q_f eH)^2}$ for different values of the magnetic field strength. In fact, we see that the free energy density seems to scale with H^2 for ($q_f = \frac{2}{3}$, $n_{\rm ext} = 1$), and ($q_f = -\frac{1}{3}$, $n_{\rm ext} = 1$), and for temperatures not too far from the critical temperature. We note, however, that in the high-temperature region physical observables are more affected by finite volume and cutoff effects. On the other hand, we see clearly that for the strongest magnetic field used in this paper ($q_f = \frac{2}{3}$, $n_{\rm ext} = 3$) the scaling with H^2 is badly violated. It is useful to give the corresponding values of the magnetic field in physical units. To this end, we use the known flavor dependence of the QCD critical temperature reported in ref. [44] to infer that for $N_f = 1$ the

JHEP12(2015)058

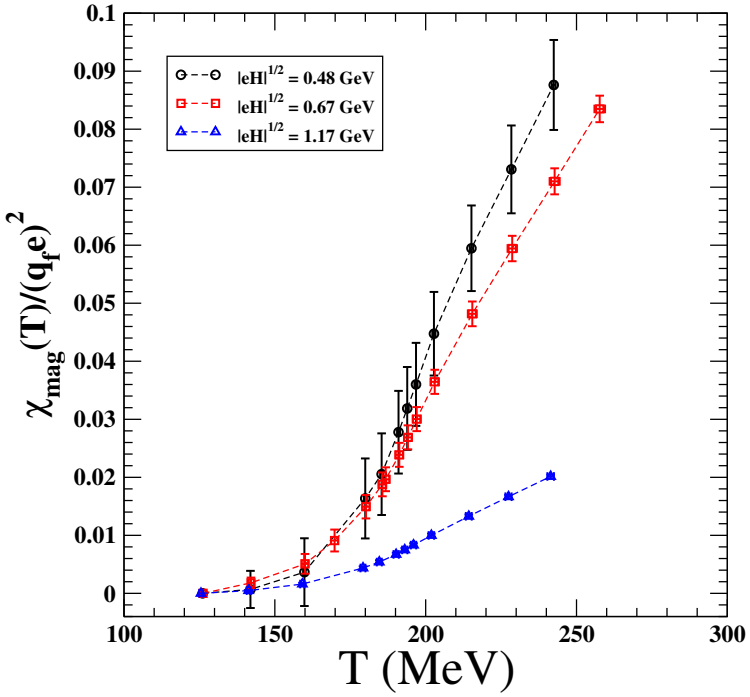

Figure 11. The magnetic susceptibility $\frac{\chi}{q_f^2 e^2}$ as a function of the temperature for different magnetic field strengths.

critical temperature is $T_c \sim 190\,\mathrm{MeV}$. This corresponds to a lattice spacing $a \simeq 0.26\,\mathrm{fm}$. So that, in the critical region, we estimate $\sqrt{|eH|} \simeq 0.48, 0.67, 1.17\,\mathrm{GeV}$ corresponding to $n_{\mathrm{ext}} = -0.5, 1, 3$ respectively. Thus, we see that for magnetic field strengths not exceeding $1.0\,\mathrm{GeV}$ the free energy density seems to display an approximate scaling with H^2 within our statistical uncertainties. This is in qualitative agreement with the results in ref. [7] where the strongest magnetic field used was $\sqrt{|eH|} \simeq 0.85\,\mathrm{GeV}$. In any case, for physical applications, we recall that the magnetic fields relevant for heavy-ion collision experiments are of order $\sqrt{|eH|} \sim 0.1\,\mathrm{GeV}$.

To determine the magnetic susceptibility we are lead to consider the free energy density for $\sqrt{|eH|} \leq 1.0\,\mathrm{GeV}$ where we can safely apply eq. (4.16). Indeed, in figure 11 we report our determination of the magnetic susceptibility as function of the temperature. For comparison, we also display our determination of the magnetic susceptibility for $\sqrt{|eH|} \simeq 1.17\,\mathrm{GeV}$. From figure 11 we see that the magnetic susceptibility is positive in the whole temperature range explored in the present study. Moreover, the magnetic susceptibility increases monotonically with the temperature. Therefore, the strongly interacting medium behaves as a paramagnetic substance both below and above the critical temperature T_c. It is remarkable that our results for the magnetic susceptibility is in fair qualitative and quantitative agreement with ref. [19] where it has been considered $N_f = 2 + 1$ QCD with physical quark masses, discretized on a lattice by stout improved staggered fermions and a tree level improved Symanzik pure gauge action.

JHEP12(2015)058

5 Conclusions and discussion

In conclusion, let us summarize briefly the main results of the present paper. We investigated QCD with one flavor of staggered quark in an external magnetic field on the lattice. The external magnetic field has been introduced by means of the so-called Schrödinger functional. We have investigated the magnetic properties of one-flavour quarks and gluons in thermal equilibrium for magnetic field strengths up to $\sqrt{|eH|} \leq 1.17\,\mathrm{GeV}$. In particular, we focused on the effects of the magnetic field on several local observables and found results in qualitative agreement with recent results in the literature obtained with a different method, as described in section 1, to implement external magnetic fields in QCD on the lattice. We have, also, looked for the effects of the magnetic field on the critical temperature. Surprisingly, we found that the critical temperature does not change even for the strongest magnetic field used in the present work. This is in striking contrast with the results in the literature. However, since we used one flavor rooted staggered quark which is known to be strongly affected by taste symmetry violation effects, one could suspect that our results on the critical temperature is merely due to lattice artifacts. Indeed, presently we are simulating the same physical system by adopting highly improved staggered quarks (HISQ) where the taste symmetry violations are dramatically reduced. Nevertheless, our preliminary simulations adopting HISQ quarks to do not yet display a clear dependence of the pseudocritical temperature on the background magnetic field. In any event, we plan to report progress on this subject in a future paper.

We evaluated the magnetic contributions to the pressure, energy density, and free energy. Our results are in qualitative agreement with previous investigations. In particular, we confirm that the free energy density scales with H^2 for small enough magnetic field strengths. Moreover, we determined the magnetic susceptibility and found that the strongly interacting medium behaves like a paramagnetic substance both below and above the critical temperature in agreement with previous results in the literature.

Acknowledgments

This work was in part based on the MILC collaboration public lattice gauge theory code, see http://www.physics.utah.edu/∼detar/milc/. This work was partially supported by the INFN SUMA project. Simulations have been performed on Blue Gene/Q Fermi and Galileo Supercomputer Cluster at CINECA (CINECA-INFN agreement), on the BC2S cluster in Bari, and on the Zefiro cluster in Pisa.

JHEP12(2015)058

References

[1] D.E. Kharzeev, K. Landsteiner, A. Schmitt and H.-U. Yee, *Strongly interacting matter in magnetic fields*, *Lect. Notes Phys.* **871** (2013) 1 [arXiv:1211.6245] [INSPIRE].

[2] G. Endrődi, *QCD in magnetic fields: from Hofstadter's butterfly to the phase diagram*, PoS(LATTICE2014)018 [arXiv:1410.8028] [INSPIRE].

[3] P.H. Damgaard and U.M. Heller, *Observation of the Meissner effect in a lattice Higgs model*, *Phys. Rev. Lett.* **60** (1988) 1246 [INSPIRE].

[4] P.H. Damgaard and U.M. Heller, *The* U(1) *Higgs model in an external electromagnetic field*, *Nucl. Phys.* **B 309** (1988) 625 [INSPIRE].

[5] P. Cea and L. Cosmai, *Constant background fields on the lattice*, *Phys. Rev.* **D 43** (1991) 620 [INSPIRE].

[6] P. Cea and L. Cosmai, *Constant background fields and unstable modes on the lattice*, *Phys. Lett.* **B 264** (1991) 415 [INSPIRE].

[7] M. D'Elia, S. Mukherjee and F. Sanfilippo, *QCD phase transition in a strong magnetic background*, *Phys. Rev.* **D 82** (2010) 051501 [arXiv:1005.5365] [INSPIRE].

[8] M. D'Elia and F. Negro, *Chiral properties of strong interactions in a magnetic background*, *Phys. Rev.* **D 83** (2011) 114028 [arXiv:1103.2080] [INSPIRE].

[9] V.V. Braguta, P.V. Buividovich, M.N. Chernodub, A.Y. Kotov and M.I. Polikarpov, *Electromagnetic superconductivity of vacuum induced by strong magnetic field: numerical evidence in lattice gauge theory*, *Phys. Lett.* **B 718** (2012) 667 [arXiv:1104.3767] [INSPIRE].

[10] E.M. Ilgenfritz, M. Kalinowski, M. Muller-Preussker, B. Petersson and A. Schreiber, *Two-color QCD with staggered fermions at finite temperature under the influence of a magnetic field*, *Phys. Rev.* **D 85** (2012) 114504 [arXiv:1203.3360] [INSPIRE].

[11] G.S. Bali et al., *The QCD phase diagram for external magnetic fields*, *JHEP* **02** (2012) 044 [arXiv:1111.4956] [INSPIRE].

[12] G.S. Bali et al., *Magnetic susceptibility of QCD at zero and at finite temperature from the lattice*, *Phys. Rev.* **D 86** (2012) 094512 [arXiv:1209.6015] [INSPIRE].

[13] G.S. Bali, F. Bruckmann, G. Endrődi, F. Gruber and A. Schaefer, *Magnetic field-induced gluonic (inverse) catalysis and pressure (an)isotropy in QCD*, *JHEP* **04** (2013) 130 [arXiv:1303.1328] [INSPIRE].

[14] C. Bonati, M. D'Elia, M. Mariti, F. Negro and F. Sanfilippo, *Magnetic susceptibility of strongly interacting matter across the deconfinement transition*, *Phys. Rev. Lett.* **111** (2013) 182001 [arXiv:1307.8063] [INSPIRE].

[15] M. D'Elia, M. Mariti and F. Negro, *Susceptibility of the QCD vacuum to CP-odd electromagnetic background fields*, *Phys. Rev. Lett.* **110** (2013) 082002 [arXiv:1209.0722] [INSPIRE].

[16] L. Levkova and C. DeTar, *quark-gluon plasma in an external magnetic field*, *Phys. Rev. Lett.* **112** (2014) 012002 [arXiv:1309.1142] [INSPIRE].

JHEP12(2015)058

[17] E.M. Ilgenfritz, M. Muller-Preussker, B. Petersson and A. Schreiber, *Magnetic catalysis (and inverse catalysis) at finite temperature in two-color lattice QCD*, *Phys. Rev.* **D 89** (2014) 054512 [arXiv:1310.7876] [INSPIRE].

[18] G.S. Bali, F. Bruckmann, G. Endrődi and A. Schäfer, *Paramagnetic squeezing of QCD matter*, *Phys. Rev. Lett.* **112** (2014) 042301 [arXiv:1311.2559] [INSPIRE].

[19] C. Bonati, M. D'Elia, M. Mariti, F. Negro and F. Sanfilippo, *Magnetic susceptibility and equation of state of $N_f = 2 + 1$ QCD with physical quark masses*, *Phys. Rev.* **D 89** (2014) 054506 [arXiv:1310.8656] [INSPIRE].

[20] V.G. Bornyakov, P.V. Buividovich, N. Cundy, O.A. Kochetkov and A. Schäfer, *Deconfinement transition in two-flavor lattice QCD with dynamical overlap fermions in an external magnetic field*, *Phys. Rev.* **D 90** (2014) 034501 [arXiv:1312.5628] [INSPIRE].

[21] G.S. Bali, F. Bruckmann, G. Endrődi, S.D. Katz and A. Schäfer, *The QCD equation of state in background magnetic fields*, *JHEP* **08** (2014) 177 [arXiv:1406.0269] [INSPIRE].

[22] S. Borsányi et al., *Full result for the QCD equation of state with $2 + 1$ flavors*, *Phys. Lett.* **B 730** (2014) 99 [arXiv:1309.5258] [INSPIRE].

[23] G. Endrődi, *Critical point in the QCD phase diagram for extremely strong background magnetic fields*, *JHEP* **07** (2015) 173 [arXiv:1504.08280] [INSPIRE].

[24] P. Cea, L. Cosmai and A.D. Polosa, *The lattice Schrödinger functional and the background field effective action*, *Phys. Lett.* **B 392** (1997) 177 [hep-lat/9601010] [INSPIRE].

[25] P. Cea, L. Cosmai and A.D. Polosa, *Finite size analysis of the* U(1) *background field effective action*, *Phys. Lett.* **B 397** (1997) 229 [hep-lat/9607020] [INSPIRE].

[26] P. Cea and L. Cosmai, *Unstable modes and confinement in the lattice Schrödinger functional approach*, *Mod. Phys. Lett.* **A 13** (1998) 861 [hep-lat/9610028] [INSPIRE].

[27] P. Cea and L. Cosmai, *Probing the nonperturbative dynamics of* SU(2) *vacuum*, *Phys. Rev.* **D 60** (1999) 094506 [hep-lat/9903005] [INSPIRE].

[28] P. Cea and L. Cosmai, *Gauge invariant study of the monopole condensation in non-Abelian lattice gauge theories*, *Phys. Rev.* **D 62** (2000) 094510 [hep-lat/0006007] [INSPIRE].

[29] P. Cea and L. Cosmai, *Probing the nonperturbative dynamics of lattice gauge theories*, *Prog. Theor. Phys. Suppl.* **138** (2000) 30 [INSPIRE].

[30] P. Cea and L. Cosmai, *Abelian monopole and vortex condensation in lattice gauge theories*, *JHEP* **11** (2001) 064 [INSPIRE].

[31] P. Cea and L. Cosmai, *External field dependence of deconfinement temperature in* SU(3), *Nucl. Phys. Proc. Suppl.* **106** (2002) 613 [hep-lat/0109030] [INSPIRE].

[32] P. Cea and L. Cosmai, *Abelian chromomagnetic fields and confinement*, *JHEP* **02** (2003) 031 [hep-lat/0204023] [INSPIRE].

[33] P. Cea and L. Cosmai, *Color dynamics in external fields*, *JHEP* **08** (2005) 079 [hep-lat/0505007] [INSPIRE].

[34] P. Cea and L. Cosmai, *Deconfinement phase transitions in external fields*, PoS(LAT2005)289 [hep-lat/0510055] [INSPIRE].

[35] P. Cea, L. Cosmai and M. D'Elia, *The deconfining phase transition in full QCD with two dynamical flavors*, *JHEP* **02** (2004) 018 [hep-lat/0401020] [INSPIRE].

JHEP12(2015)058

[36] P. Cea, L. Cosmai and M. D'Elia, *QCD dynamics in a constant chromomagnetic field*, *JHEP* **12** (2007) 097 [arXiv:0707.1149] [INSPIRE].

[37] P. Cea, L. Cosmai, P. Giudice and A. Papa, *Chiral symmetry breaking in planar QED in external magnetic fields*, *Phys. Rev.* **D 85** (2012) 094505 [arXiv:1204.6112] [INSPIRE].

[38] http://www.physics.utah.edu/∼detar/milc/.

[39] T. DeGrand and C. DeTar, *Lattice methods for quantum chromodynamics*, World Scientific (2006) [INSPIRE].

[40] G. Endrődi, *QCD equation of state at nonzero magnetic fields in the hadron resonance gas model*, *JHEP* **04** (2013) 023 [arXiv:1301.1307] [INSPIRE].

[41] K. Kamikado and T. Kanazawa, *Magnetic susceptibility of a strongly interacting thermal medium with* $2+1$ *quark flavors*, *JHEP* **01** (2015) 129 [arXiv:1410.6253] [INSPIRE].

[42] P. Elmfors, D. Persson and B.-S. Skagerstam, *QED effective action at finite temperature and density*, *Phys. Rev. Lett.* **71** (1993) 480 [hep-th/9305004] [INSPIRE].

[43] L.D. Landau and E.M. Lifshitz, *Electrodynamics of continuous media*, Pergamon Press (1984).

[44] F. Karsch, E. Laermann and A. Peikert, *Quark mass and flavor dependence of the QCD phase transition*, *Nucl. Phys.* **B 605** (2001) 579 [hep-lat/0012023] [INSPIRE].

JHEP12(2015)058